RSC Sustainability

ROYAL SOCIETY OF CHEMISTRY

PAPER

View Article Online
View Journal | View Issue

Cite this: *RSC Sustainability*, 2025, **3**, 2366

Ruthenium-catalyzed dimerization of vanillin for the formation of a biobased epoxy thermoset resin†

Flavia Ferrara, [a] Iuliana Ribca, [b] Namratha Prabhu, ‡[a] Josselin Mante, ‡[a] Maureen Gumbo, [a] Andreas Ekebergh, *[a] Mats Johansson *[b] and Nina Kann *[a]

Received 6th March 2025
Accepted 9th April 2025

DOI: 10.1039/d5su00165j

rsc.li/rscsus

Vanillin is one of few lignin platform chemicals that are currently available on industrial scale. Seeking to find biobased alternatives to the reprotoxic compound bisphenol A (BPA), we have successfully dimerized three different monomeric vanillin derivatives in a ruthenium-catalyzed Tischenko reaction. The resulting esters were characterized by NMR, FTIR, HRMS, and single crystal X-ray diffraction. The thermal behaviour of one of these derivatives, the epoxy divanillin ester **EDVE**, was studied further by DSC and TGA. **EDVE** was subsequently applied towards the preparation of an epoxy thermoset resin *via* curing with Jeffamine D-400. The thermoset formulation was thermally cured, monitoring the curing with DSC and FTIR. The final thermoset was then characterized with respect to physical and mechanical properties with DSC, TGA, and DMA. This catalytic approach provides a new strategy to access vanillin-based epoxides that could potentially replace bisphenol A.

Sustainability spotlight

The transition to a sustainable industry requires not only the replacement of precursors derived from petroleum with biomass alternatives, but also that current chemical processes adapt to accommodate the oxygenated structures of biobased molecules. Ideally, toxic chemicals should be exchanged for more benign alternatives, and catalytic, rather than stoichiometric, methods should be used. Vanillin is one of few biobased aromatic platform chemicals that is currently accessible on industrial scale. Striving to find a replacement for reprotoxic bisphenol A (BPA), we here report the catalytic dimerization of a vanillin-based monomer, as well as the application of the resulting ester in an epoxy thermoset. This work aligns with the UN Sustainable Development Goal 12 – Responsible consumption and production.

Introduction

Bisphenol A (BPA, Fig. 1) is a common monomer used in polymeric materials such as polycarbonates and epoxy resins, and also in thermal papers and food packaging.[1] However, BPA displays reproductive toxicity by causing endocrine disruption, and replacements for this monomer are thus urgently needed.[2] In addition, current production of BPA affords toxic byproducts[3] and the precursors are generally derived from fossil resources.[4] Recent reports show that a methoxy substituent on one or both of the phenol rings of BPA can significantly reduce the estrogenic activity,[5,6] making lignin-based aromatics well suited as precursors for BPA substitutes.[3,7]

One of the most important platform chemicals from lignin is vanillin, which is also one of very few aromatic biobased precursors that is accessible on an industrial scale.[8] Caillol and co-workers have exploited this versatile precursor in the synthesis of a variety of vanillin-based monomers for use in biobased polymers.[9] Fig. 1 shows one such structure, the diglycidyl ether of vanillin alcohol (**DGEVA**),[9,10] which was employed in the synthesis of biobased epoxy thermosets.[10,11]

DGEVA has also been used in conjunction with biobased anhydrides to form thermally stable epoxy resins for the aerospace sector, as reported by Mija.[12] To mimic the diaryl structure of bisphenol A, the dimerization of vanillin has been implemented using different strategies. Pearl and colleagues used electrochemical coupling for this purpose as early as 1952,[13,14] and this methodology was later optimized by Harvey *et al.*, who incorporated the prepared vanillin bisphenols into polycyanurates and polycarbonates.[15] Epoxy resins prepared *via* electrochemical vanillin dimerization have been reported by Amarasekara.[16] Another approach is to oxidatively couple vanillin or vanillyl alcohol *via* the aromatic ring to form a dimeric structure (**GEDVA** or **EDV**, Fig. 1), a tactic applied by Cramail,[17] as well as Fang and Nejad,[18] to prepare biobased

[a]*Department of Chemistry and Chemical Engineering, Chalmers University of Technology, SE-412 96 Göteborg, Sweden. E-mail: kann@chalmers.se*

[b]*KTH Royal Institute of Technology, Department of Fibre and Polymer Technology, Division of Coating Technology, SE-100 44 Stockholm, Sweden. E-mail: matskg@kth.se*

† Electronic supplementary information (ESI) available. CCDC 2371862 and 2423529. For ESI and crystallographic data in CIF or other electronic format see DOI: https://doi.org/10.1039/d5su00165j

‡ These authors contributed equally to this work.

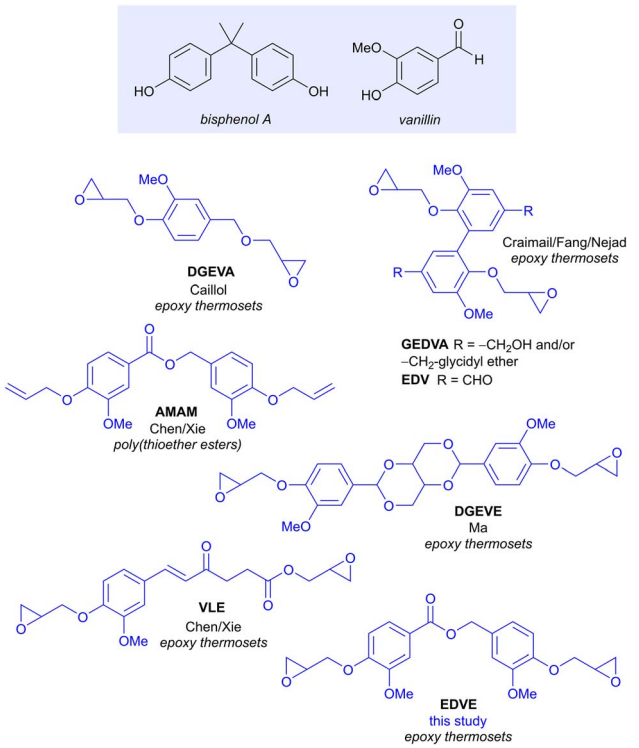

Fig. 1 Selected vanillin-based monomers for polymerization and their areas of application.

epoxy thermoset resins. The aldehyde functionality of vanillin can also be exploited for coupling reactions, for instance *via* reaction with a diol/polyol or with a diamine. A degradable diepoxy monomer (**DGEVE**, Fig. 1), with two vanillin units linked *via* a central bicycloacetal deriving from erythritol, was reported by Ma and colleagues.[19] **DGEVE** showed excellent degradability in acidic solutions after use, but was found to be stable under neutral conditions. Coupling a diamine to two equivalents of vanillin *via* imine formation is another approach to prepare bisphenol compounds, as described by Desnoes,[20] as well as Li and Zeng.[21] The corresponding vanillin-based diimines were subsequently applied towards the formation of biobased epoxy thermosets and vitrimers.

The base-catalyzed dimerization of aldehydes to produce an ester, originally reported by Claisen in 1887,[22] but generally known as the Tishchenko reaction,[23–25] provides another means for dimerizing vanillin. Chen and Xie applied this strategy with good results in the dimerization of allylated vanillin using sodium hydride as the catalyst, forming a divanillin ester (**AMAM**, Fig. 1).[26] **AMAM** was subsequently employed in thiol-ene click reactions and acyclic diene metathesis, to produce poly(thioether esters) and polyesters with high molecular weight. Thermoset thiol-ene networks were prepared by the same group,[27] and Du and Zhu later applied **AMAM** towards polyurethane thermosets.[28] Chen and Xie have also exploited the vanillin aldehyde functionality in another type of coupling reaction *i.e.* the aldol condensation between vanillin and platform chemical levulinic acid, forming the bio-based building block **VLE** (Fig. 1).[29] **VLE** was cured with an aromatic diamine, to form an imine-containing epoxy resin with improved thermal stability and mechanical properties compared to a bisphenol A epoxy resin. Xie has described the synthesis of a vanillin-based bisphenol carbonate and its application in the synthesis of polycarbonate esters and urethanes,[30] while Llevot employed a divanillin carbonate in reactions with a myrcene-derived trithiol to prepare acid-degradable biobased polycarbonates *via* photopolymerization.[31] Liu reported the synthesis of a bisguaiacol amide and ester and studied their material performances and cytotoxicity.[32] Structures that more closely resemble BPA have also been prepared by Stanzione and colleagues, by coupling vanillyl alcohol with guaiacol under acidic conditions.[33] The resulting bisguaicol structure was subsequently converted to a diglycidyl ether and applied in epoxy thermoset resins. Some recent reviews provide a comprehensive summary the use of vanillin building blocks in BPA replacements and in biobased polymers.[34–36]

While the base-catalyzed Tischenko reaction proceeds smoothly for dimerizing allylated vanillin into the corresponding ester, as reported by Chen and Xie,[26] the basic reaction conditions used may be too harsh for more sensitive functionalities such as epoxides, that are commonly used in polymerization. In addition, sodium hydride is incompatible with certain solvents,[37] and may be less suited for large-scale industrial scale applications due its pyrophoric nature.[38] An alternative here could be to use transition metal catalysis for aldehyde dimerization under milder reaction conditions. Shvo has shown that catalytic dimerization of both aliphatic and aromatic aldehydes to form the corresponding esters can be catalyzed by a Shvo-type ruthenium complex.[39] Darses has also reported that *in situ* generated ruthenium catalysts, prepared from $[RuCl_2(p\text{-cymene})]_2$ and different phosphine ligands, can be applied for the same purpose.[40] As part of studies in our respective groups, involving hydrogen transfer reactions using platform chemicals from biomass,[41,42] as well as the preparation of polymers from renewable resources (vegetable oils,[43] terpenes,[44] suberin,[45] and lignin[46]), we investigated the ruthenium-catalysed dimerization of vanillin and derivatives thereof to form biobased esters for polymer applications. We subsequently applied one of these compounds, the epoxy divanillin ester **EDVE**, towards the preparation of an epoxy thermoset resin. The results of these studies are disclosed herein.

Results and discussion

Synthesis of vanillin epoxy dimers *via* ruthenium-catalyzed coupling

Several different vanillin derivatives were investigated in the ruthenium-catalyzed coupling reaction to form vanillin epoxy dimers. In addition to vanillin itself, two derivatives where the phenol functionality was protected as an acetate or a silyl ether, were also prepared in case the free phenol functionality should interfere with the catalyst activity. Vanillin (**1a**, Scheme 1) was reacted with acetic anhydride, using 4-dimethylaminopyridine (DMAP) as a catalyst,[47] to produce acetylated vanillin **1b** in 98% yield. To form the silyl-protected derivative **1c**, vanillin was

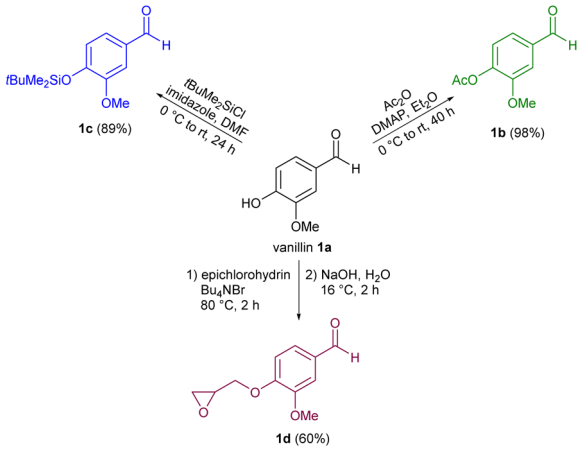

Scheme 1 Preparation of vanillin monomer building blocks **1b–1d**.

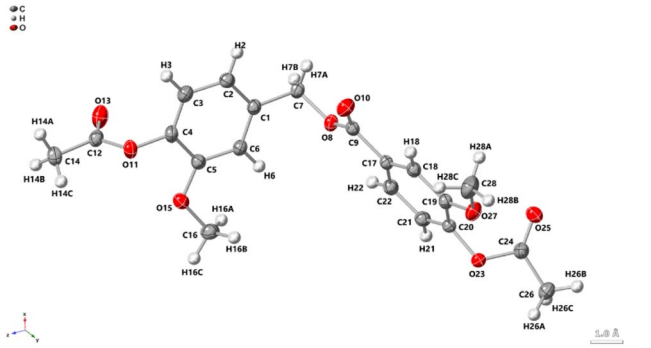

Fig. 2 Solid state structure of compound **2b**. Ellipsoids are represented at 50% probability. H atoms are shown as spheres of arbitrary radius. CCDC 2371862.

instead treated with *tert*-butyldimethylsilyl chloride in the presence of imidazole,[48] to afford the desired compound in 89% yield. Given the sensitivity of the epoxy group, we initially planned to perform the ruthenium-catalyzed coupling reaction using either unprotected vanillin, or one of the derivatives **1b** or **1c**, to form a diester, and subsequently introduce the epoxide functionality after dimerization. A different strategy, however, could be to investigate the direct dimerization of derivative **1d**, where the epoxy functionality is present already at the start. To form the precursor needed for such a reaction, vanillin was reacted with epichlorohydrin in the presence of tetrabutylammonium bromide, under solventless conditions at 80 °C,[49,50] affording **1d** as a white solid in 60% yield.

Direct coupling vanillin itself using 1.25 mol% of the Shvo catalyst **3** in the presence of formic acid under solventless conditions did not afford the desired coupling product **2a**, despite heating for several days (Scheme 2). Deactivation of the catalyst *via* coordination to the phenolic group may be involved here. To see if this was indeed the case, we instead turned to the acetyl-protected derivative **1b**. Initial attempts to dimerize **1b** with the Shvo catalyst under solventless conditions, using a reaction time of 20 hours at 100 °C under argon, did indeed afford the desired ester **2b**. However, the conversion seemed to plateau at around 50–60%. A similar trend was reported by Shvo in the case of electron rich aldehydes such as *p*-methoxybenzaldehyde.[39] Postulating that catalyst deactivation or degradation was occurring, we added one portion of catalyst at the start of the reaction, together with a small amount of toluene to solubilize the starting material, and subsequently a second portion of catalyst after 20 hours, using 2.5 mol% catalyst in total. The reaction was then heated for an additional 20 hours. To our delight, ester **2b** could be isolated in up to 70% yield following purification by automated flash chromatography on silica gel, using a gradient of ethyl acetate in pentane as the solvent. The structure of ester **2b** was verified by ^{1}H and ^{13}C NMR, IR, HRMS (see Experimental section), and X-ray crystallography (Fig. 2).

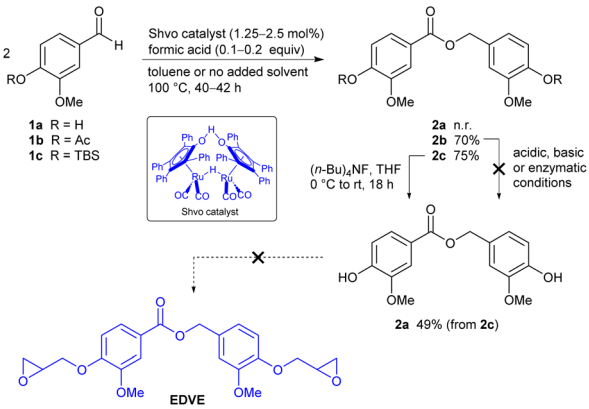

Scheme 2 Initial strategy to prepare **EDVE**.

The next step would be to deprotect the acetate in order to install the epoxy functionality. However, selective cleavage of the acyl ester in **2b**, in the presence of the newly installed central ester functionality, proved to be challenging, despite the investigation of basic, acidic and enzymatic (porcine lipase) cleavage conditions, resulting in either disproportionation of the benzyl ester or low conversion to product. Reasoning that a silyl ether might be more facile to cleave in the presence of the central ester functionality, the dimerization of TBS-protected vanillin **1c** was performed. As the precursor **1c** is an oil rather than a solid in this case, no toluene was added and the reaction was performed under solventless conditions. In addition, a lower amount of catalyst (1.25 mol%) was needed in comparison to the earlier experiment. The resulting ester **2c** was found to be difficult to separate from small amounts of residual **1c** on a silica column, but switching to a reversed phase column (C18), afforded pure **2c** in 75% yield. Cleavage of the silyl protecting group in **2c** using tetrabutylammonium fluoride (TBAF) in THF afforded unprotected dimer **2a** in a moderate yield (49%, non-optimized). However, subjecting **2a** to the basic conditions needed for derivatizing the phenolic groups with epichlorohydrin again resulted in decomposition, and the initial strategy was thus abandoned.

We had earlier refrained from using vanillin derivatized with an epoxy group already at the start, due to the sensitivity of this functionality. However, we now decided to investigate if vanillin

Table 1 Ruthenium-catalyzed dimerization of **1d** to **EDVE**

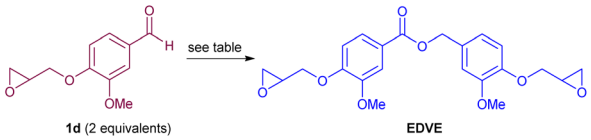

1d (2 equivalents) **EDVE**

Entry	Catalyst[a] (mol%)	HCOOH[b] or HCOONa[c] (mol%)	Solvent (mL per mmol per vanillin)	Time (h)	Conv.[d] (%)
1	Shvo (2.5)	20	No solvent	48	70
2	Shvo (2.5)	20	Toluene (0.6)	48	81
3	Shvo (3.75)	20	Toluene (0.4)	36	89
4	Shvo (3.75)	20	Toluene (0.4)	72	88
5	Shvo (5)	20	Toluene (0.4)	96	92
6[e]	$[RuCl_2(p\text{-cym})]_2$ (2.5)	15	1,4-Dioxane (1)	16	<5
7[e]	$[RuCl_2(p\text{-cym})]_2$ (2.5)	15	1,4-Dioxane (0.2)	16	<5

[a] Catalyst added in 1.25 mol% portions, see Experimental section for details. [b] HCOOH used in entries 1–5. [c] HCOONa used in entries 6–7. [d] Conversion determined by ^{1}H NMR of the crude product. [e] 5 mol% $CyPPh_2$ added.

epoxide derivative **1d** (Scheme 1) was compatible with the ruthenium-catalyzed coupling, as this would provide a more direct route to the targeted epoxy divanillin ester **EDVE**. The results from this investigation are summarized in Table 1. While **1d** is a solid, its relatively low melting point (80 °C) prompted us to initially investigate solventless conditions. The conversion was determined by ^{1}H NMR of the crude product by comparing the aldehyde signal of **1d** to the benzyl peak in **2d**, after filtering the reaction mixture through neutral alumina to remove the catalyst. Using 2.5 mol% catalyst, added in two portions over 48 h, a promising 70% conversion of vanillin epoxide **1d** to **EDVE** was obtained (Table 1, entry 1). However, we noticed that some of the aldehyde **1d** sublimated upon heating and resolidified onto the walls of the vial, thus being removed from the reaction mixture. Adding a small amount of toluene proved to solve this issue, resulting in 81% conversion to dimer, still employing 2.5% mol of catalyst with a reaction time of 48 h (Table 1, entry 2). To see if the conversion could be improved even further, we added additional portions of catalyst and experimented with the reaction time. With 3.75 mol% catalyst, added in three portions, essentially the same conversion (88–89%) was obtained after 36 h and after 72 h (entries 3 and 4). A slightly higher conversion (92%) could be obtained using 5 mol% catalyst with a reaction time of 96 h. However, the conditions used in entry 3 provide a more optimized balance of catalyst amount and reaction time.

We also briefly investigated dimerization conditions reported by Simon and Darses,[40] where a different ruthenium catalyst, $[RuCl_2(p\text{-cym})]_2$, together with an added ligand ($CyPPh_2$), were used to generate an active catalytic species *in situ*. While the authors report a high conversion of aromatic aldehydes to dimerized product, this methodology was not successful for the epoxy-functionalized substrate **1d**, leaving the starting material essentially untouched (Table 1, entries 5 and 6). It may be that the high oxygen content of this particular substrate interferes with the catalyst under these reaction conditions in some way.

After obtaining a satisfactory conversion in the formation of **EDVE**, we then focused on purification of the crude product, where the main contaminant is unreacted **1d**. Automated flash chromatography was found to be inefficient, as the majority of the product was trapped on the silica gel and only a small amount of product (<10%) could be eluted using ethyl acetate in pentane, albeit in high purity. By switching to a C18-column, using a gradient of H_2O–MeOH as the eluent, the product was successfully eluted, initially in yields of 40–52%. However, with some optimization of the eluent, a 65% yield of pure **EDVE** could be achieved. For characterization purposes, we have aimed to isolate pure **EDVE**, resulting in some material loss on the C18 column. However, related studies on vanillin-containing epoxy dimers in many cases employ the crude product directly in the preparation of epoxy resins,[18,20,51] without further purification. As a conversion in the range of 89–92% (Table 1) can be attained under the optimized conditions, with the main contaminant being unreacted **1d**, an alternative for larger scale reactions could be to use the crude material directly in the epoxy resin synthesis. Overall, this direct coupling method provides a shorter route to **EDVE** than our initial strategy, by removing the protection/deprotection steps.

Characterization and thermal behaviour of EDVE

EDVE was characterized by ^{1}H NMR, ^{13}C NMR, HRMS, ATR FTIR and single crystal X-ray diffraction. ^{1}H NMR clearly shows the transition from an aldehyde proton at 9.86 ppm in **1d** (Fig. 3a, peak h) to a benzylic ester peak at 5.27 ppm in **EDVE** (peak i), with new peaks appearing in both the aromatic (6.9–7.7 ppm) and aliphatic (2.7–4.4 ppm) area in **EDVE**, corresponding to an additional aromatic ring and epoxide functionality compared to **1d**. In addition, the spectra for **EDVE** displays two -OMe signals at 3.91 and 3.89 ppm, compared to only one -OMe peak at 3.93 ppm in the case of **1d**. In ^{13}C NMR (Fig. 3b), the carbonyl signal for the aldehyde at 191 ppm disappears and is replaced by the ester carbonyl at 166 ppm, also verifying the formation of **EDVE**. HRMS analysis also corresponds to the correct mass for **EDVE** (see Experimental section).

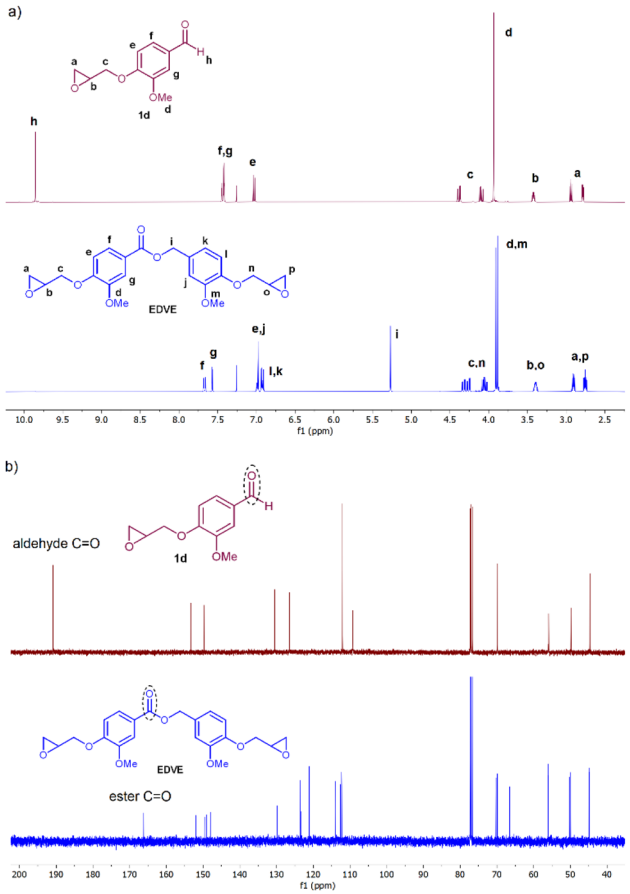

Fig. 3 (a) ^{1}H NMR spectrum of vanillin epoxide **1d** (top) and **EDVE** (bottom) in $CDCl_3$; (b) ^{13}C NMR spectra of vanillin epoxide **1d** (top) and **EDVE** (bottom) in $CDCl_3$.

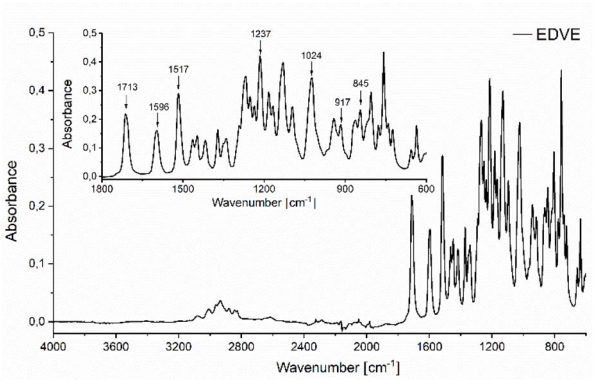

Fig. 4 ATR FTIR spectrum of **EDVE**.

The ATR FTIR spectrum of **EDVE** is shown in Fig. 4, where the absorption signals at 917 and 845 cm^{-1} are assigned to the oxirane ring,[52] while the signals at 1596 and 1517 cm^{-1} represent the aromatic C=C stretching vibration.[53] The signals at 1024 and 1237 cm^{-1} arise from the methoxy group,[54] while the absorption band at 1713 cm^{-1} can be attributed to the stretching vibration of the ester carbonyl group.[55] In comparison, the aldehyde carbonyl of **1d** appears at 1683 cm^{-1}.[56] The shift of this carbonyl signal to a higher wavelength is consistent with the conversion of an aromatic aldehyde, typically with its C=O stretch in the 1685–1710 cm^{-1} region, to an aromatic ester, which generally appears in the 1705–1725 cm^{-1} range.[57] Single crystal X-ray diffraction (Fig. 5) provides additional proof of the **EDVE** structure.

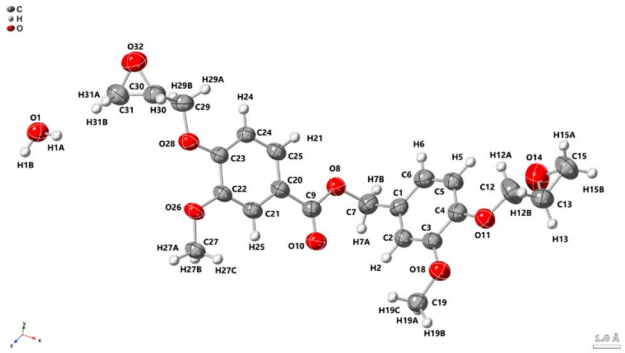

Fig. 5 X-ray crystallographic structure of **EDVE** with thermal ellipsoids at 50% probability. H atoms are shown as spheres of arbitrary radius. CCDC 2423529.

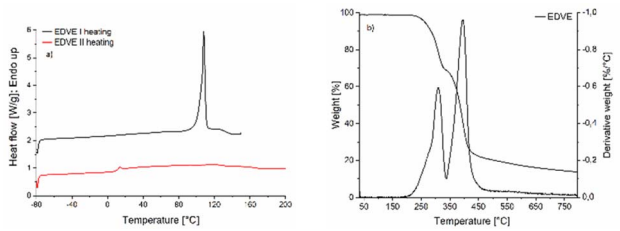

Fig. 6 Thermal behaviour of **EDVE** studied by (a) DSC and (b) TGA/DTGA.

The thermal behaviour of **EDVE** was studied by DSC and TGA The DSC analysis shown in Fig. 6a revealed a semi-crystalline structure, with the first heating curve presenting the endotherm corresponding to the melting point of **EDVE** with a maximum at 108 °C. During cooling from the melt, no recrystallization event was observed. The absence of recrystallization at lower temperatures is proposed to be due to limited molecular mobility and time for recrystallization during cooling. There is a small transition at 11 °C seen on the second heating corresponding to a T_g transition meaning that below this temperature is the system in the vitrified state where no crystallization can occur. The thermal decomposition of **EDVE** was studied by TGA and derivative TGA analysis. Fig. 6b shows that the decomposition of **EDVE** takes place in two steps. The first step is located between 203–338 °C with 31% mass loss and the maximum degradation rate peak in the DTGA at 309 °C, while the second step can be found between 338–442 °C with 79% mass loss and the maximum at 397 °C. The results suggest that the first degradation is coupled to the aryl–alkyl ether linkage that first breaks to split off a glycidyl group and then the ester linkage is broken at higher temperatures.

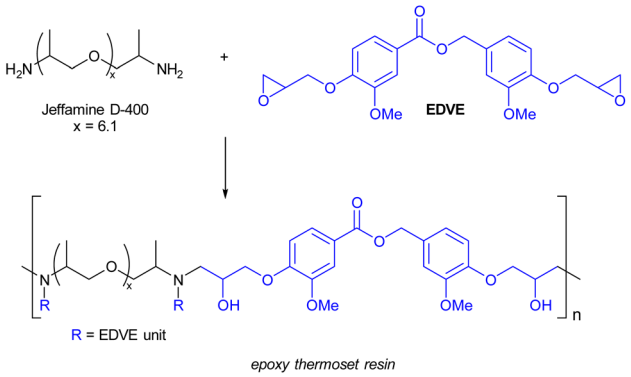

Scheme 3 Epoxy thermoset prepared from **EDVE** and Jeffamine D-400.

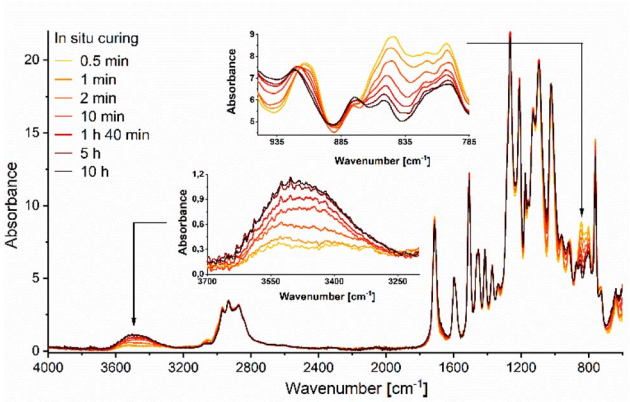

Fig. 8 Real-time ATR FTIR analysis of the curing of **EDVE** with Jeffamine D-400 at 140 °C.

Synthesis of a vanillin epoxy thermoset resin from EDVE and Jeffamine D-400

The curing process of **EDVE** and Jeffamine D-400 (Scheme 3) was studied by DSC in order to choose the optimum curing temperature. Fig. 6a and 7a show the DSC thermograms of **EDVE** and Jeffamine D-400 respectively, where it is seen that **EDVE** is semi-crystalline with a melting point at 108 °C, while the Jeffamine is amorphous. In Fig. 7b, the heat-flow data as a function of temperature for a sample which was mixed 45 minutes before the measurement, using a small amount of acetone as a co-solvent, is displayed. This waiting period was necessary to allow for a partial evaporation of acetone and ensure minimum impact on the thermal behavior of the curing process. The first heating curve presents an endothermic maximum at 82 °C (melting point of **EDVE** = 108 °C) and two exothermic maxima at 129 °C and 168 °C. Two maxima can indicate the two main stages of the reaction. The second heating curve shows a T_g of 45 °C and a completely cured thermoset (no visible exotherm). This curing behaviour is in line with the corresponding system based on a BPA-based epoxy previously studied.[58]

The spectral evolution at 140 °C of the curing process of **EDVE** with Jeffamine D-400 was also studied by real-time ATR FTIR, as seen in Fig. 8. A curing temperature of 140 °C was selected to prevent degradation or evaporation of the monomers. *In situ* DSC measurements of the reaction between **EDVE** and Jeffamine D-400 revealed two exothermic maxima at 129 °C and 168 °C, indicating that a higher curing temperature, such as 170 °C, could accelerate the reaction. Thermogravimetric analysis (TGA) of Jeffamine D-400 showed a 5 wt% weight loss at 155 °C, and considering the vapor pressure of 1 mm Hg per °C at 165 °C, temperatures around 170 °C could lead to monomer evaporation/degradation. While a higher curing temperature could have accelerated the reaction, 140 °C was chosen as an optimal compromise between curing efficiency and avoiding monomer evaporation/degradation.

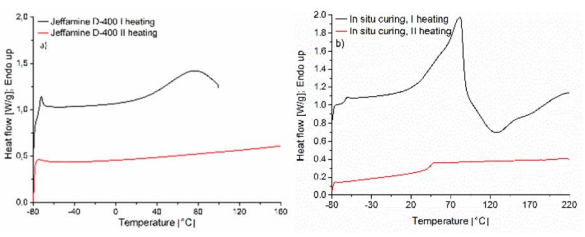

Fig. 7 DSC thermogram of (a) Jeffamine D-400, and (b) **EDVE** and Jeffamine D-400 during the curing process. See Fig. 5a for a DSC thermogram of **EDVE** only.

The signals at 917 and 845 cm^{-1} are drastically reduced already after 10 minutes, and continue to decrease over several hours, with significant changes observed between 10 minutes and 5 h. The changes between 5 h and 10 h are minimal, which indicated that the reaction is almost completed and the epoxy groups consumed. In order to accelerate the reaction, the curing temperature can be further increased. Simultaneously, the signal corresponding to the OH vibrational stretching at ~3500 cm^{-1} is increasing, indicating that a ring-opening reaction of the oxirane ring is occurring during the curing process.[52] The combined results from the FTIR and DSC measurements confirm that **EDVE** works well as an alternative to the corresponding BPA-based epoxy.

The resulting epoxy network was also characterized by TGA and DSC, as shown in Fig. 9. The resulting thermoset has a thermal stability up to 300 °C where the degradation starts. This is very similar to the thermal stability of the corresponding BPA-based epoxy system.[58] Comparing the TGA results for the monomers (Fig. 6b and 9a) and the final thermoset (Fig. 9b), one can see that the thermal stability is improved for the thermoset, being at least 60 °C higher compared to the thermal stability of the monomers, which is in line with the previous discussion. Additionally, the T_g of the epoxy thermosets is around 47 ± 2.6 °C, which aligns well with the DSC data obtained during the *in situ* curing process. This significant increase in T_g from around 11 °C for the **EDVE** monomer to 47 °C for the thermoset further confirms the formation of a cross-linked network during curing, with the final T_g in the typical range for a system based on Jeffamine D-400. BPA-based epoxy systems combined with Jeffamine D-400 normally have a T_g around 50 ± 5 °C and an elastic modulus around 2 GPa.[58,59]

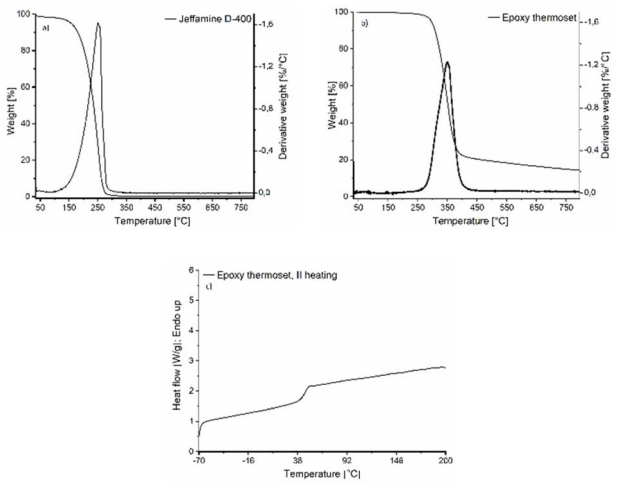

Fig. 9 TGA of (a) Jeffamine D-400, and (b) epoxy thermoset prepared from **EDVE** and Jeffamine D-400. (c) DSC of the epoxy thermoset.

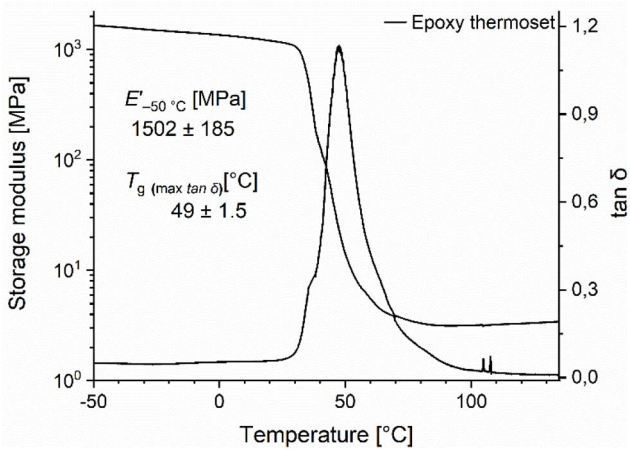

Fig. 10 DMA of epoxy thermoset prepared from **EDVE** and Jeffamine D-400.

In Fig. 10, the DMA data of the epoxy thermoset is shown. The storage modulus at −50 °C is around 1502 ± 185 and drops significantly around the glass transition temperature which is around 49 ± 1.5 °C, providing a good correlation between the T_g measured by DSC and DMA.

Conclusions

In summary, we have developed a convenient ruthenium-catalyzed synthetic route to the epoxy divanillin ester **EDVE**, where the target compound is formed in a single step from the corresponding vanillin epoxide derivative. The reaction is highly atom economic, with all atoms in the precursor vanillin epoxide being incorporated into the product. **EDVE** was characterized by NMR, FTIR, HRMS and single crystal X-ray diffraction, and subsequently applied in the synthesis of an epoxy thermoset resin *via* curing with Jeffamine D-400. The properties of the resulting resin were investigated using DSC, TGA and DMA, showing that the thermoset exhibited good thermal stability and physical and mechanical properties suitable for thermoset applications, in par with corresponding BPA-epoxy system. Our initial results indicate that biobased **EDVE** could potentially function as a replacement to BPA-based epoxy. In addition, the introduction of an ester moiety into the epoxy resin structure could facilitate recycling of the polymer by chemical or enzymatic hydrolysis after use. We envisage that **EDVE** can be a valuable addition to the current collection of biobased building blocks for polymer applications.

Experimental section

Materials

Vanillin (**1a**, 99%) was purchased from Sigma Aldrich. The Shvo catalyst (1-hydroxytetraphenylcyclopentadienyl-(tetraphenyl-2,4-cyclopentadien-1-one)-μ-hydrotetracarbonyl-diruthenium-(II)) was purchased from Strem. Jeffamine D-400 polyetheramine was purchased from Huntsman. All other solvents and reagents were purchased from commercial suppliers and used without purification or drying, unless otherwise stated. Microwave reaction vials with caps were purchased from Biotage. Reactions were heated using a Radleys Heat-On Block in conjunction with an IKA magnetic stirrer/heater.

Analytical methods

Nuclear magnetic resonance spectroscopy (NMR). ^{1}H NMR and ^{13}C NMR, were recorded on an Agilent 400 MHz (101 MHz for ^{13}C NMR). The chemical shifts for ^{1}H and ^{13}C NMR spectra are reported in parts per million (ppm) using the residual solvent peak for reference ($CDCl_3$, 7.26 ppm). The following abbreviations are used for reporting NMR peaks: singlet (s), doublet (d), triplet (t), quartet (q), multiplet (m), and apparent (app). All coupling constants (J) are reported in Hertz (Hz). The acquired spectra were processed using MestReNova v14.2.0-26256 (Mestrelab Research S.L. 2020).

Fourier transform infrared spectroscopy (FTIR) and real time FTIR (RT-FTIR). ATR-FTIR spectra of monomers **1b–d** and dimers **2a–c** were recorded on a PerkinElmer Spectrum Frontier instrument with a pike-GladiATR module. A PerkinElmer Spectrum 100 system with an attenuated total reflection (ATR) accessory, equipped with a diamond crystal, and a temperature control unit (Specac, Heated Golden Gate Controller) was used to characterize **EDVE** and Jeffamine D-400 and also to follow *in situ* curing of the epoxy thermoset. FTIR spectra were acquired at room temperature, by averaging 16 scans, from 4000 to 600 cm^{-1}, with a resolution of 4 cm^{-1}. For the real-time FTIR measurements, a drop of the resin solution was added to a pre-heated ATR accessory, (previously described in the experimental section, synthesis of an epoxy thermoset from **EDVE**). The solution was first left in the fume hood for 1 h to allow the acetone to evaporate. RT-FTIR measurements were performed at 140 °C and a new scan was acquired every 30 s. All RT-FTIR spectra were normalized to the 15 96 cm^{-1} signal, corresponding to the aromatic C=C stretching vibration, and baseline corrected by using Spectrum software.[52] The curing reaction was followed by

monitoring the decrease in RT-FTIR absorption intensity of the oxirane ring absorption (917 and 845 cm^{-1})[42] add the increase in hydroxyl (–OH) absorption around 3500 cm^{-1}.

Differential scanning calorimetry (DSC). DSC thermograms of **EDVE**, Jeffamine D-400, and epoxy thermosets were recorded using a Mettler Toledo DSC1 instrument. Approximately 5–10 mg of each sample was placed in a 100 μL aluminum crucible, covered with a pierced lid. The **EDVE** and epoxy thermoset samples were first heated to 150 °C, while Jeffamine D-400 was heated to 100 °C, with both temperatures maintained for 10 minutes. This first heating cycle was performed to remove the thermal history of the samples. All samples were then cooled to −80 °C and kept for 10 minutes before being re-heated to 200 °C at a rate of 10 °C min^{-1}. All heating and cooling cycles were done under nitrogen atmosphere, with a flow rate of 50 mL min^{-1}. The glass transition temperature (T_g) was determined as the midpoint of the second heating run. Additionally, *in situ* curing of the epoxy thermoset was performed. The same procedure was used as for the **EDVE** sample, with the only difference being that the sample for the *in situ* curing was heated up to 220 °C instead of 200 °C. The same sample preparation was followed as for the RT-FTIR measurements.

Melting points. Melting points for monomers **1** and dimers **2** were recorded on a Büchi Melting Point B-545 apparatus or on a Mettler FP82 HT Hot Stage, equipped with an FP90 Central Processor and an Olympus BH-2 microscope.

Thermogravimetric analysis (TGA). TGA were conducted using a Mettler Toledo TGA/DSC1 instrument. **EDVE**, Jeffamine D-400, and epoxy thermoset samples, of approximately 5–10 mg each, were placed in 70 μL ceramic crucibles. Initially, the samples were heated to 30 °C and held for 10 minutes. Subsequently, they were heated to 800 °C and maintained at this temperature for an additional 10 minutes. The heating rate was set at 5 °C min^{-1}, with a nitrogen flow rate of 50 mL min^{-1}.

Dynamic mechanical analysis (DMA). DMA were recorded using a TA Instruments Q800 in tensile mode. The epoxy thermosets (10 mm × 5.2 mm × 0.10 mm) were cooled to −5 °C and held for 5 minutes. After that, they were heated to 150 °C at a rate of 3 °C min^{-1}. The preload force was set to 0.01 N, with a force track of 125%, a frequency of 1 Hz, and a strain of 0.1%. Storage modulus (E') and tan δ were continuously recorded as a function of temperature. The T_g of the thermosets was reported as maximum of the tan δ curve.

High-resolution mass spectrometry (HRMS). HRMS was performed on an Agilent 1290 infinity LC system equipped with an autosampler tandem to an Agilent 6520 Accurate Mass Q-TOF LC/MS.

X-ray diffraction (XRD). Single crystals of **2b** were obtained by recrystallisation from methanol and **EDVE** single crystals were obtained by recrystallisation from MeOH : H_2O : EtOAc (1 : 0.5 : 0.5). Suitable crystals were selected and placed on a mounted cryo loop and mounted on an XtaLAB Synergy R, HyPix diffractometer. The crystal was kept at a steady T = 145.07(10) K for **2b** and T = 153(5) K for **EDVE** during data collection. The structures were solved with the ShelXT46 (ref. 60) structure solution program using the Intrinsic Phasing solution method and by using Olex247 (ref. 61) as the graphical interface. The model was refined with version 2016/6 of ShelXL 2016/646 (ref. 61) using Least Squares minimisation. The data was submitted to the CSD with deposition numbers CCDC 2371862 (**2b**) and CCDC 2423529 (**EDVE**).

Synthetic procedures and polymerization methods

Automated flash chromatography was performed on a Biotage Isolera Spektra One with SNAP KP-sil or KP-C18-HS columns, or on a Biotage Selekt with Sfär Silica D or Sfär C18 D columns, eluting with EtOAc–pentane (silica) or H_2O–MeOH (C18). Conventional flash chromatography using glass columns may also be used for purification of the products.

Synthesis of 4-formyl-2-methoxyphenyl acetate (1b). Vanillin (**1a**, 500 mg, 3.29 mmol, 1 equiv.) and 4-dimethylaminopyridine (DMAP, 0.5 mg, 4 μmol, 0.1 mol%) were dissolved in diethyl ether (2 mL) in a capped 5 mL Biotage reaction vial equipped with a stir bar. The suspension was stirred and acetic anhydride (465 μL, 4.93 mmol, 1.5 equiv.) was added dropwise. The solution became clear and was stirred at 20 °C for 40 h. The solution was diluted with diethyl ether (10 mL) and washed with water (10 mL). The aqueous phase was extracted with diethyl ether (3 × 25 mL). The combined organic phases were dried over Na_2SO_4 and concentrated under rotary evaporation, affording **1b** as white crystals (628 mg, 98%). Analytical data are in accordance with published data for this compound.[62]

Synthesis of 4-((*tert*-butyldimethylsilyl)oxy)-3-methoxybenzaldehyde (1c). Compound **1c** was prepared using a modification of a procedure reported by Iwabuchi and co-workers.[47] Vanillin (**1a**, 500 mg, 3.29 mmol, 1 equiv.) and imidazole (290 mg, 4.27 mmol, 1.3 equiv.) were dissolved in 2 mL DMF in a capped 5 mL Biotage reaction vial equipped with a stir bar. The flask was flushed with nitrogen and cooled to 0 °C. *tert*-Butyldimethylsilyl chloride (594 mg, 3.94 mmol, 1.2 equiv.) was added in one portion, the vial was capped again and the clear colourless reaction was stirred for 5 min at 0 °C, whereupon the ice bath was removed and the reaction was stirred at room temperature for 24 h. The reaction was quenched with 25 mL aqueous NH_4Cl (satd), extracted with diethyl ether (3 × 25 mL), washed with brine (2 × 25 mL), dried over Na_2SO_4 and concentrated under rotary evaporation. The crude product was purified by automated flash chromatography (silica, 0–10% EtOAc in petroleum ether), affording **1c** as a pale yellow oil (776 mg, 89%). ^{1}H NMR and IR data are in accordance with published data for this compound.[48] ^{13}C NMR (101 MHz, chloroform-d) δ 191.1, 151.6, 151.3, 130.9, 126.3, 120.7, 110.0, 55.4, 25.6, 18.5, −4.

Synthesis of 3-methoxy-4-(oxiran-2-ylmethoxy)benzaldehyde (1d). A modification of procedures reported by Zhao *et al.*[49] and Wang *et al.*[50] was used. Vanillin (**1a**, 5.00 g, 32.9 mmol, 1 equiv.) was added to a 100 mL round bottom flask equipped with a stir bar. Epichlorohydrin (10.3 mL, 131 mmol, 4 equiv.) was added, followed by tetrabutylammonium bromide (254 mg, 0.789 mmol, 0.02 equiv.). The flask was equipped with a water-cooled condenser and heated at 80 °C, whereupon the initially formed slurry became a clear pale yellow solution. After 2 h, the heating was turned off and the solution was cooled to 16 °C

using a water bath with a small amount of ice. An aqueous solution of NaOH (3.29 g NaOH in 5.3 mL water) was added dropwise over 15 min, whereupon the solution became a thick slurry. Water (10 mL) was added and the flask was shaken every 15 min for 2 h. The slurry was diluted with 50 mL EtOAc and filtered through a glass frit (NS3). The filter cake was rinsed with an additional 2 × 50 mL EtOAc and the combined organic phases were washed with water (3 × 75 mL), dried over Na_2SO_4 and concentrated under rotary evaporation, affording **2d** as a white solid (4.08 g, 60%). Analytical data are in accordance with published data for this compound.[50]

Synthesis of 4-acetoxy-3-methoxybenzyl 4-acetoxy-3-methoxybenzoate (2b). 2.5 mol% catalyst was used in this experiment, divided into two portions. 4-Formyl-2-methoxyphenyl acetate (**1b**, 388 mg, 2 mmol) was placed in a 5 mL Biotage microwave reaction vial, together with an initial portion (27 mg, 1.25 mol%) of the Shvo catalyst **3**. The vial was capped, placed under argon. Toluene (0.5 mL) and degassed formic acid (22 μL, 0.4 mmol) was added. The vial was heated to 100 °C using a heating block, whereupon the initially formed heterogeneous mixture converted to a clear solution. A second portion of the catalyst (27 mg, 1.25 mol%) was added after 18 h and the reaction was heated for an additional 24 h. The product was purified by automated flash chromatography, using a gradient of 1–40% EtOAc in petroleum ether, affording 290 mg (70%) of **2b** as a grey-white crystalline solid. Mp 89–90 °C; ν_{max}/cm^{-1} (neat) 1756 (C═O), 1717 (C═O), 1191 (C–O); ^{1}H NMR (400 MHz, $CDCl_3$) δ 7.70 (dd, J = 8.1, 1.8 Hz, 1H), 7.66 (app d, J = 1.8 Hz, 1H), 7.10 (app d, J = 8.1 Hz, 1H), 7.06–7.00 (m, 3H), 5.32 (s, 2H), 3.88 (s, 3H), 3.84 (s, 3H), 2.32 (s, 3H), 2.31 (s, 3H); ^{13}C NMR (101 MHz, $CDCl_3$) δ 169.0, 168.5, 165.7, 151.1 (2C), 143.7, 139.7, 134.8, 128.6, 122.9, 122.8, 122.7, 120.7, 113.5, 112.4, 66.6, 56.1, 55.9, 20.6 (2C); HRMS (ESI$^+$) m/z: [M + Na]$^+$ calcd for $C_{20}H_{20}NaO_8$ 411.1056; found 411.1054.

Synthesis of 4-((*tert*-butyldimethylsilyl)oxy)-3-methoxybenzyl 4-((*tert*-butyldimethylsilyl)oxy)-3-methoxybenzoate (2c). 1.25 mol% catalyst was used in this experiment, divided into two portions. 4-((*tert*-Butyldimethylsilyl)oxy)-3-methoxybenzaldehyde (**1c**, 417 mg, 1.57 mmol) was placed in a 5 mL Biotage microwave reaction vial, together with an initial portion (9.7 mg, 0.57 mol%) of the Shvo catalyst **3**. The vial was capped, placed under argon. Degassed formic acid (6 mL, 0.1 mmol) was added. The vial was heated to 100 °C using a heating block, whereupon the initially formed heterogeneous mixture converted to a clear solution. A second portion of the catalyst (11.5 mg, 0.68 mol%) was added after 20 h and the reaction was heated for an additional 22 h. The crude product was purified by automated flash chromatography on a C18 column, eluting with H_2O : MeOH (40 : 60 → 0 : 100). The last fraction afforded the product as a colourless viscous oil (312 mg, 0.59 mmol, 75%); ν_{max}/cm^{-1} (neat) 1713 (C═O), 1277 (C–O); ^{1}H NMR (400 MHz, $CDCl_3$) δ 7.60 (dd, J = 8.2, 2.0 Hz, 1H), 7.56 (app d, J = 2.0 Hz, 1H), 6.94–6.88 (m, 2H), 6.85 (app t, J = 8.2 Hz, 2H), 5.25 (s, 2H), 3.85 (s, 3H), 3.82 (s, 3H), 0.994 (s 9H), 0.988 (s, 9H), 0.16 (s, 6H), 0.15 (s, 6H); ^{13}C NMR (101 MHz, $CDCl_3$) δ 166.4, 150.9, 150.7, 149.7, 145.1, 129.6, 123.7, 123.4, 121.2, 120.8, 120.4, 113.1, 112.5, 66.6, 55.5 (2C), 25.7 (3C), 25.6 (3C), 18.5 (2C), 18.4 (2C), −4.6 (2C); HRMS (ESI$^+$) m/z: [M + Na]$^+$ calcd for $C_{28}H_{44}NaO_6Si_2$ 555.2574; found 555.2573. This reaction has also been performed using 11.3 mmol of **1c**, affording **2c** in 71% yield.

Deprotection of 2c to form 4-hydroxy-3-methoxybenzyl 4-hydroxy-3-methoxybenzoate (vanillin dimer 2a). TBS-protected vanillin dimer **2c** (1.04 g, 1.95 mmol, 1 equiv.) dissolved in THF (12 mL) was added to a 100 mL round bottom flask equipped with a stir bar. The flask was cooled to 0 °C, whereupon tetrabutylammonium fluoride (3.08 g, 9.76 mmol, 5 equiv.) was added in portions. The reaction was allowed to warm to room temperature while stirring for 18 h. The reaction mixture was diluted with 50 mL water, extracted with EtOAc (3 × 50 mL) and the combined extracts were washed with water (50 mL), dried over Na_2SO_4 and concentrated under rotary evaporation. The crude product was purified by automated flash chromatography (0–80% EtOAc in petroleum ether, product eluting around 60% EtOAc), affording 289 mg (0.95 mmol, 49%) of **2a** as a yellow solid (non-optimized). Analytical data are in accordance with published data for this compound (prepared *via* a different route).[32]

Synthesis of 3-methoxy-4-(oxiran-2-ylmethoxy)benzyl 3-methoxy-4-(oxiran-2-ylmethoxy)benzoate (EDVE). 3.75 mol% catalyst was used in this experiment, divided into three portions. 3-Methoxy-4-(oxiran-2-ylmethoxy)benzaldehyde **1d** (416 mg, 2.00 mmol) was placed in a 5 mL Biotage microwave reaction vial, together with an initial portion (27 mg, 1.25 mol%) of the Shvo catalyst **3**. The vial was capped and placed under argon. Degassed toluene (0.8 mL) and degassed formic acid (15 μL, 0.40 mmol) were then added. The vial was heated to 100 °C using a heating block, whereupon the initially formed yellow slurry converted to a clear orange solution. Two additional 27 mg portions of catalyst **3** were added over a 24 h period. After additional 15 h, the reaction mixture was allowed to cool to ambient temperature, filtered through a plug of neutral alumina, eluting with EtOAc, and the solution was concentrated. The crude product was purified by automated flash chromatography on a Biotage C18 column, eluting with H_2O : MeOH (0 → 70% MeOH). The second fraction afforded the product as a white solid (270 mg, 65%); mp 108 °C; ν_{max}/cm^{-1} (neat) 1708 (C═O), 1270 (C–O); ^{1}H NMR (400 MHz, $CDCl_3$) δ 7.67 (dd, J = 8.4, 2.1 Hz, 1H), 7.57 (app d, J = 2.0 Hz, 1H), 7.01–6.96 (m, 2H), 6.94–6.90 (m, 2H), 5.27 (s, 2H), 4.32 (dd, J = 11.4, 3.2 Hz, 1H), 4.26 (dd, J = 11.4, 3.4 Hz, 1H), 4.07 (dd, J = 11.4, 5.6 Hz, 1H), 4.04 (dd, J = 11.5, 5.6 Hz, 1H), 3.91 (s, 3H), 3.89 (s, 3H), 3.42–3.37 (m, 2H), 2.91 (ddd, J = 6.7, 4.9, 4.1 Hz, 2H), 2.75 (ddd, J = 7.3, 4.9, 2.6 Hz, 2H); ^{13}C NMR (101 MHz, $CDCl_3$) δ 166.2, 152.0, 149.6, 149.0, 148.0, 129.8, 123.5, 123.4, 121.1, 113.9, 112.6, 112.3, 112.2, 70.2, 69.8, 66.6, 56.0 (2C), 50.1, 50.0, 44.9, 44.8; HRMS (ESI$^+$) m/z: [M + H]$^+$ found 417.1548; calcd for $C_{22}H_{25}O_8$ 417.1549. Some decomposition of **EDVE** was seen in halogenated solvents and longer term storage in such solvents is thus not recommended.

Synthesis of an epoxy thermoset from EDVE. Jeffamine D-400 (15.5 mg) and **EDVE** (30.0 mg) were weighed into a glass vial and dissolved in 1 mL of acetone by shaking under vortex mixing. The mixture was poured into a silicon mold and placed in a fume hood for 1 h to allow evaporation of the solvent. The mixture was subsequently cured in an oven at 140 °C for 10 h to

form the epoxy thermoset from **EDVE**. The free-standing samples were removed from the silicon mold and stored in closed glass vials. The samples dimensions were ≈10 mm × 5.2 mm × 0.10 mm.

Data availability

The ^{1}H and ^{13}C NMR data supporting this article has been included as part of the ESI.† Crystallographic data for **2b** and **EDVE** has been deposited at the CCDC under 2371862 (for **2b**) and 2423529 (for **EDVE**) and can be obtained from **https://www.ccdc.cam.ac.uk/structures/**.

Author contributions

F. F. and I. R.: investigation, validation, writing – review & editing. N. P. and J. M.: investigation. M. G.: investigation, formal analysis, writing – review & editing. A. E., M. J. and N. K.: conceptualization, methodology, supervision, funding acquisition, resources, writing – original draft.

Conflicts of interest

A. E. is an employee of AstraZeneca and may or may not own stock options. There are no other conflicts of interest to declare.

Acknowledgements

Financial support from the Swedish Research Council Formas (NK, grant no. 2015-01106), the C. F. Lundström Foundation (NK, grant no. CF2021-0027), the Adlerbertska Foundation (NK) and the Knut and Alice Wallenberg Foundation (KAW) through the Wallenberg Wood Science Center (MJ) is gratefully acknowledged.

References

1 J. Michalowicz, *Environ. Toxicol. Pharmacol.*, 2014, **37**, 738–758.
2 J. S. Siracusa, L. Yin, E. Measel, S. X. Liang and X. Z. Yu, *Reprod. Toxicol.*, 2018, **79**, 96–123.
3 F. Liguori, C. Moreno-Marrodan and P. Barbaro, *Chem. Soc. Rev.*, 2020, **49**, 6329–6363.
4 Y. Jiang, J. Li, D. Li, Y. K. Ma, S. C. Zhou, Y. Wang and D. H. Zhang, *Chem. Soc. Rev.*, 2024, **53**, 624–655.
5 Y. Peng, K. H. Nicastro, T. H. Epps and C. Q. Wu, *Food Chem.*, 2021, **338**, 127656.
6 A. Amitrano, J. S. Mahajan, L. T. J. Korley and T. H. I. Epps, *RSC Adv.*, 2021, **11**, 22149–22158.
7 R. Tavernier, M. Semsarilar and S. Caillol, *Green Mater.*, 2023, **12**, 121–167.
8 M. Fache, B. Boutevin and S. Caillol, *ACS Sustain. Chem. Eng.*, 2016, **4**, 35–46.
9 M. Fache, E. Darroman, V. Besse, R. Auvergne, S. Caillol and B. Boutevin, *Green Chem.*, 2014, **16**, 1987–1998.
10 M. Fache, R. Auvergne, B. Boutevin and S. Caillol, *Eur. Polym. J.*, 2015, **67**, 527–538.
11 A. S. Mora, R. Tayouo, B. Boutevin, G. David and S. Caillol, *Green Chem.*, 2018, **20**, 4075–4084.
12 R. Dinu, U. Lafont, O. Damiano and A. Mija, *ACS Appl. Polym. Mater.*, 2022, **4**, 3636–3646.
13 I. A. Pearl, *J. Am. Chem. Soc.*, 1952, **74**, 4593–4594.
14 I. A. Pearl, *J. Am. Chem. Soc.*, 1952, **74**, 4260–4262.
15 B. G. Harvey, A. J. Guenthner, H. A. Meylemans, S. R. L. Haines, K. R. Lamison, T. J. Groshens, L. R. Cambrea, M. C. Davis and W. W. Lai, *Green Chem.*, 2015, **17**, 1249–1258.
16 A. S. Amarasekara, R. Garcia-Obergon and A. K. Thompson, *J. Appl. Polym. Sci.*, 2019, **136**, 47000.
17 E. Savonnet, E. Grau, S. Grelier, B. Defoort and H. Cramail, *ACS Sustain. Chem. Eng.*, 2018, **6**, 11008–11017.
18 Z. Fang, S. Nikafshar, E. L. Hegg and M. Nejad, *ACS Sustain. Chem. Eng.*, 2020, **8**, 9095–9103.
19 W. C. Yuan, S. Q. Ma, S. Wang, Q. Li, B. B. Wang, X. W. Xu, K. F. Huang, J. Chen, S. S. You and J. Zhu, *Eur. Polym. J.*, 2019, **117**, 200–207.
20 E. Desnoes, L. Toubal, A. H. Bouazza and D. Montplaisir, *Polym. Eng. Sci.*, 2020, **60**, 2593–2605.
21 P. X. Tian, Y. D. Li, Y. X. Weng, Z. Hu and J. B. Zeng, *Eur. Polym. J.*, 2023, **193**, 112078.
22 L. Claisen, *Ber. Dtsch. Chem. Ges.*, 1887, **20**, 646–650.
23 V. E. Tishchenko, *J. Russ. Phys.-Chem. Soc.*, 1906, **38**, 355–418.
24 V. E. Tischenko, *Chem. Zentralbl.*, 1906, **77**, 1309–1311.
25 T. Seki, T. Nakajo and M. Onaka, *Chem. Lett.*, 2006, **35**, 824–829.
26 T. H. Ren, Q. Chen, C. B. Zhao, Q. Zheng, H. B. Xie and M. North, *Green Chem.*, 2020, **22**, 1542–1547.
27 Z. J. Gao, Y. You, Q. Chen, M. North and H. B. Xie, *Green Chem.*, 2023, **25**, 172–182.
28 D. Zhao, X. Liang, J. W. Wang, J. Z. Du and Y. Q. Zhu, *ACS Appl. Polym. Mater.*, 2023, **5**, 4536–4545.
29 Z. T. Cao, Y. You, Y. Q. Li, C. J. Huang, Y. Z. Tian, S. H. Zhao, Q. Chen and H. B. Xie, *Polym. Chem.*, 2023, **14**, 3978–3988.
30 D. Bai, Q. Chen, Y. Chai, T. H. Ren, C. J. Huang, I. D. V. Ingram, M. North, Q. Zheng and H. B. Xie, *RSC Adv.*, 2018, **8**, 34297–34303.
31 P. S. Löser, A. Lamouroux, M. A. R. Meier and A. Llevot, *Polym. Chem.*, 2024, **15**, 2240–2252.
32 H. R. Sun, J. Y. Jiang, Y. L. Zheng, S. F. Xiang, S. J. Zhao, F. Y. Fu and X. D. Liu, *Polym. Chem.*, 2023, **14**, 1613–1621.
33 E. D. Hernandez, A. W. Bassett, J. M. Sadler, J. J. La Scala and J. F. Stanzione, *ACS Sustain. Chem. Eng.*, 2016, **4**, 4328–4339.
34 H. R. Qiang, J. W. Wang, H. X. Liu and Y. Q. Zhu, *Polym. Chem.*, 2023, **14**, 4255–4274.
35 M. A. Rashid, M. N. Hasan, M. A. R. Dayan, M. S. I. Jamal and M. K. Patoary, *Reactions*, 2023, **4**, 66–91.
36 W. J. Yang, H. Ding, D. Puglia, J. M. Kenny, T. X. Liu, J. Q. Guo, Q. W. Wang, R. X. Ou, P. W. Xu, P. M. Ma and P. J. Lemstra, *SusMat*, 2022, **2**, 535–568.
37 Q. Yang, M. Sheng, J. J. Henkelis, S. Y. Tu, E. Wiensch, H. L. Zhang, Y. Q. Zhang, C. Tucker and D. E. Ejeh, *Org. Process Res. Dev.*, 2019, **23**, 2210–2217.

38 C. Fluegeman, T. Hilton, K. P. Moder and R. Stankovich, *Process Saf. Prog.*, 2005, **24**, 86–90.
39 N. Menashe and Y. Shvo, *Organometallics*, 1991, **10**, 3885–3891.
40 M. O. Simon and S. Darses, *Adv. Synth. Catal.*, 2010, **352**, 305–308.
41 A. Said Stålsmeden, J. L. B. Vázquez, K. van Weerdenburg, R. Rae, P. O. Norrby and N. Kann, *ACS Sustain. Chem. Eng.*, 2016, **4**, 5730–5736.
42 A. Ekebergh, R. Begon and N. Kann, *J. Org. Chem.*, 2020, **85**, 2966–2975.
43 K. Ohlsson, T. Bergman, P. E. Sundell, T. Deltin, I. Tran, M. Svensson and M. Johansson, *Prog. Org. Coat.*, 2012, **73**, 291–293.
44 M. Claudino, J. M. Mathevet, M. Jonsson and M. Johansson, *Polym. Chem.*, 2014, **5**, 3245–3260.
45 S. Nameer and M. Johansson, *J. Coat. Technol. Res.*, 2017, **14**, 757–765.
46 M. Jawerth, M. Lawoko, S. Lundmark, C. Perez-Berumen and M. Johansson, *RSC Adv.*, 2016, **6**, 96281–96288.
47 S. Nagasawa, S. Fujiki, Y. Sasano and Y. Iwabuchi, *J. Org. Chem.*, 2021, **86**, 6952–6968.
48 T. Schneider, V. Kubyshkin and N. Budisa, *Eur. J. Org Chem.*, 2018, **2018**, 2053–2063.
49 S. Zhao and M. M. Abu-Omar, *Macromolecules*, 2018, **51**, 9816–9824.
50 S. Wang, S. Q. Ma, Q. Li, X. W. Xu, B. B. Wang, W. C. Yuan, S. H. Zhou, S. S. You and J. Zhu, *Green Chem.*, 2019, **21**, 1484–1497.
51 M. Fache, B. Boutevin and S. Caillol, *Green Chem.*, 2016, **18**, 712–725.
52 M. G. González, J. C. Cabanelas and J. Baselga, in *Infrared Spectroscopy - Materials Science, Engineering and Technology*, ed. T. Theophanides, InTech, Rijeka, 2012, ch. 13, pp. 261–284.
53 Z. Y. Wang, P. Gnanasekar, S. S. Nair, R. Farnood, S. L. Yi and N. Yan, *ACS Sustain. Chem. Eng.*, 2020, **8**, 11215–11223.
54 V. Balachandran and K. Parimala, *Spectrochim. Acta, Part A*, 2012, **95**, 354–368.
55 C. C. Pang, J. Zhang, Q. F. Zhang, G. L. Wu, Y. N. Wang and J. B. Ma, *Polym. Chem.*, 2015, **6**, 797–804.
56 X. M. Ding, L. Chen, Y. J. Xu, X. H. Shi, X. Luo, X. Song and Y. Z. Wang, *ACS Sustain. Chem. Eng.*, 2023, **11**, 14445–14456.
57 P. Larkin, in *Infrared and Raman Spectroscopy : Principles and Spectral Interpretation*, Elsevier, Waltham, UK, 2011, ch. 6, pp. 73–116.
58 D. Ratna, S. B. Jagtap, R. Nimje and B. C. Chakraborty, *J. Therm. Anal. Calorim.*, 2024, **149**, 1073–1087.
59 B. Burton, D. Alexander, H. Klein, A. Garibay-Vasquez, A. Pekarik and C. Henkee, Epoxy formulations using Jeffamine polyether-amines, *Technical Report*, Huntsman, 2005.
60 G. M. Sheldrick, *Acta Crystallogr., Sect. C:Struct. Chem.*, 2015, **71**, 3–8.
61 O. V. Dolomanov, L. J. Bourhis, R. J. Gildea, J. A. K. Howard and H. Puschmann, *J. Appl. Crystallogr.*, 2009, **42**, 339–341.
62 K. Sommer and R. M. Williams, *Tetrahedron*, 2009, **65**, 3246–3260.